Case Studies in Thermal Engineering 6 (2015) 226–237

Contents lists available at ScienceDirect

Case Studies in Thermal Engineering

journal homepage: www.elsevier.com/locate/csite

Thermal and optical efficiency investigation of a parabolic trough collector

C. Tzivanidis, E. Bellos *, D. Korres, K.A. Antonopoulos, G. Mitsopoulos

National Technical University of Athens, School of Mechanical Engineering, Thermal Department, Heroon Polytehniou 9, Zografou, 157 73 Athens, Greece

ARTICLE INFO

Article history:
Received 7 October 2015
Received in revised form
18 October 2015
Accepted 18 October 2015
Available online 10 November 2015

Keywords:
Parabolic trough collector
Heat convection coefficient
Thermal efficiency
Solidworks
Local concentration ratio
Optical efficiency

ABSTRACT

Solar energy utilization is a promising Renewable Energy source for covering a variety of energy needs of our society. This study presents the most well-known solar concentrating system, the parabolic trough collector, which is operating efficiently in high temperatures. The simulation tool of this analysis is the commercial software Solidworks which simulates complicated problems with an easy way using the finite elements method. A small parabolic trough collector model is designed and simulated for different operating conditions. The goal of this study is to predict the efficiency of this model and to analyze the heat transfer phenomena that take place. The efficiency curve is compared to a one dimensional numerical model in order to make a simple validation. Moreover, the temperature distribution in the absorber and inside the tube is presented while the heat flux distribution in the outer surface of the absorber is given. The heat convection coefficient inside the tube is calculated and compared with the theoretical one according to the literature. Also the angle efficiency modifier is calculated in order to predict the thermal and optical efficiency for different operating conditions. The final results show that the PTC model performs efficiently and all the calculations are validated.

1. Introduction

Fossil fuel depletion and global warming problem lead our society to the use of clean and abundant energy sources. Renewable energy sources are sustainable by producing zero greenhouse gas emissions and will be always available, so they seem to be the most suitable energy sources for the future. Solar energy is the oldest energy source ever used and is widely used by giving solutions in many applications, from industrial hot water supply to electricity production [1–4], especially in countries with a high solar irradiation level as Greece [5,6]. More specifically, concentrated solar collectors are able to produce high temperatures (over 400 °C) with high thermal efficiency. This is the fact that makes them a feasible and promising technology for solar desalination, solar chemistry applications, solar cooling (absorption and adsorption), solar hydrogen production and of course for Concentrated Solar Plants (CSP) [7].

The main solar technologies for electricity production are Linear Fresnel collectors, parabolic dish combined with a Stirling engine, parabolic trough collectors and solar tower (central receiver system) [8,9]. Parabolic trough collectors (PTC) cover the 90% of the total CSP systems [10] because this technology is the most mature among the concentrating collectors; it leads to light structure systems and is applied since decades [11]. Nowadays, many commercial CSP systems are operating

* Corresponding author.
E-mail address: bellose@central.ntua.gr (E. Bellos).

http://dx.doi.org/10.1016/j.csite.2015.10.005

Nomenclature

A	area, m^2
C_L	local concentration ratio
c_p	specific heat capacity, kJ/kg K
D	diameter, m
F_R	heat removal factor
F'	collector efficiency factor
F''	flow efficiency factor
G_b	solar beam radiation, W/m^2
h	convection coefficient, W/m^2K
k	thermal conductivity, W/m K
K	Angle efficiency modifier
L	tube length, m
m	mass flow rate, kg/s
Nu	mean Nusselt number
Pr	Prandtl number
Q	Heat flux, W
Re	Reynolds number
T	Temperature, K
U_L	Losses coefficient, W/m^2K
W	Width, m

Greek symbols

β	peripheral absorber angle, °
ε	emittance
η	efficiency
θ	angular displacement in longitudinal direction, °
μ	dynamic viscosity, Pa s
ρ	reflectance
σ	Stefan–Boltzmann constant [$=5.67 \cdot 10^{-8}$ W/m^2 K^4]
$(\tau\alpha)$	transmittance–absorptance product

Subscripts and superscripts

a	aperture
abs	absorbed
am	ambient
c	cover
ca	Cover-ambient
ci	inner cover
co	outer cover
fm	Mean fluid
in	inlet
loss	losses
m	mean
opt	optical
out	outlet
r	receiver
ri	inner receiver
ro	outer receiver
s	Solar
u	useful

in countries with high solar energy potential, as U.S.A. [12], Algeria [13,14] and Spain [15]. The basic parts of a PTC are an evacuated tube and a linear parabolic reflector. The reflector is made by bending a reflecting material into a parabolic shape and the evacuated tube is located in the focus line of this parabola. The main idea of this technology is the reflection of the solar beam radiation from the parabolic reflector towards to the evacuated tube in order to heat the working fluid. The general efficiency improvements and the cost reduction of PTC systems are essential factors for the further development of CSP systems worldwide [9,16]. Thus, many researches have been working in this field trying new ideas and optimizing the existing collectors [17,18].

According to the literature, a great amount of parameters that influence the PTC′s efficiency have been studied with numerical models and simulations tools. Wind influence on thermal efficiency is examined by Hachicha et al. [19] while extended optical analysis of concentrating collector is studied by many researchers, with Cheng et al. to use the Monte Carlo ray-tracing optical model in order to simulate a PTC [20] and Binotti et al. [10] to use FirstOPTIC method to calculate the optical analysis of the examined models. Ouagued et al. [16] solved a system of energy balance differential equations with Euler method and made an analysis for the influence of HTF price on the thermal energy cost. The use of synthetic oil nanofluid as the working fluid is studied by Sokhansefat et al. [21] and de Risi et al. [18] with the final results to conclude that the use of nanoparticles increases the heat transfer coefficient between the absorber and the working fluid.

In thermal performance studies, the majority of numerical studies use one dimensional heat transfer analysis [22–25] which is the simplest numerical method. Marif et al. [26] by using this method concluded that liquid water performs better than synthetic oil (TherminolVP-1™). Gong et al. [25] made both one and three dimension heat transfer analysis and proved that the two methods agree with the test results. Also, three dimensional studies are available in the literature [27–30]. Xu et al. [31] developed a dynamic model in order to study the performance of a PTC in transient operations and tested it with experimental data. Many other simulations have been developed with Engineering Equations Solver (EES) and have been validated with existing results [32–34]. On the other hand, simulations with well-known software exist in literature. Tsai and Lin [35] used Solidworks to simulate different kinds of reflectors for a PTC collector in order to maximize the thermal efficiency. Akbarimoosavi and Yaghoubi [36] used ANSYS and concluded that the high thermal conductive absorber materials lead the reduction of maximum peripheral temperature difference and so the thermal efficiency increases. Moreover, FLUENT is a very useful tool for simulations and many works have been met in bibliography [37–39]. The simulation by Mwesigye et al. [40] has a great interest because proves that the use of perforated plate inserts inside the tube increases the thermal efficiency by 1.2% with significant reduction in the absorber temperature. Also, many experimental works with numerical validation are available in the literature [41–46].

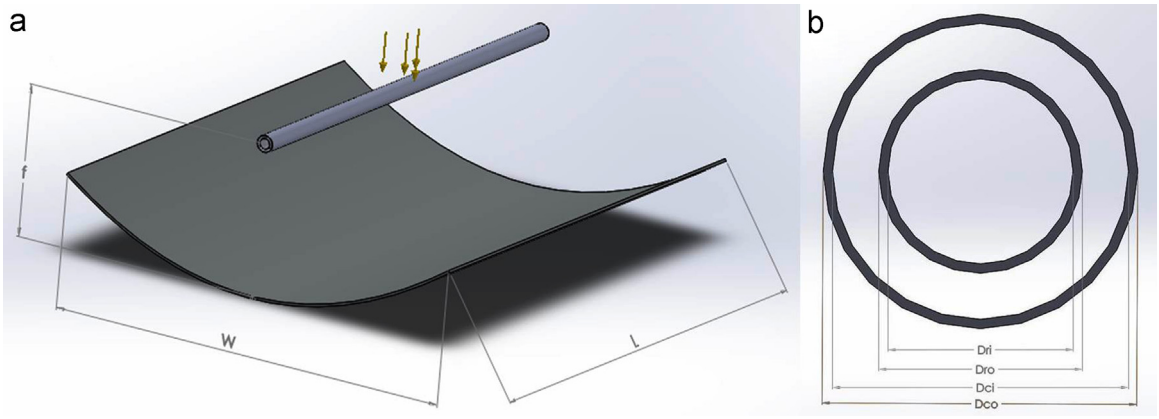

Fig. 1. Parabolic trough collector model designed in Solidworks, (a) trough dimensions (b) evacuated tube dimensions.

In this study, a parabolic trough collector is investigated with the commercial software Solidworks in order to analyze the efficiency performance in different operating conditions. The model takes into consideration all the observing phenomena including radiation heat transfer, convection heat transfer, conduction heat transfer and solar beam radiation reflections in order to simulate the collector performance successfully. Furthermore, a simple 1-D thermal model is developed to validate the simulation results from Solidworks.

2. Simulation model and analysis

The simulation of a parabolic trough collector is the aim of this study. For this reason, a small model designed and analyzed in Solidworks in order to reduce the computational time. These results are able to be generalized for a greater model with similar concentration ratio.

2.1. PTC model description

The parabolic trough collector designed in Solidworks and after analyzed in Flow Simulation Studio. Fig. 1a shows the examined model and Fig. 1b explains the dimensions of the evacuated tube.

The main dimensions of this model, while important parameters of the simulation are given in Table 1. Typical values are considered for the heat transfer parameters in order to simulate realistic conditions.

The left column of the Table 1 gives the simulation parameters and the right column contains the basic dimensions of the model. All these parameters have constant values in all examined cases. The inlet temperature and the solar incident angle in the longitude direction are the parameters that change in order to simulate different operating conditions. The working fluid in this analysis is pressurized water which remains in liquid phase in all cases. A pressure over 20 bar (saturation temperature close to 200 °C) is needed in order to keep water in liquid phase. The water inlet temperature varies from 10 to 180 °C in order to examine a great range of cases.

2.2. Mathematical presentation

In this part the basic mathematical equations of this analysis are given. First of all, the useful energy can be calculated by Eq. (2.1) and solar energy in the trough aperture by Eq. (2.2). It is important to state that a PTC utilizes only the beam radiation of the sun.

Table 1
Model dimensions and simulation parameters.

Simulation parameters	**Value**	**Model dimensions**	**Value** (m)
ε_p	0.1	W	0.840
ε_c	0.88	L	1.000
$\rho(\tau\alpha)$	0.8015	f	0.300
G_b	500 W/m^2	D_{ri}	0.020
m	0.02 kg/s	D_{ro}	0.022
T_{am}	10 °C	D_{ci}	0.032
h_{ca}	10 W/m^{2}K	D_{co}	0.034

$$Q_u = \dot{m}\cdot c_p\cdot\left(T_{out} - T_{in}\right), \tag{2.1}$$

$$Q_s = A_a\cdot G_b, \tag{2.2}$$

By combining these equations, the thermal efficiency of the collector is calculated as:

$$\eta = \frac{Q_u}{Q_s}, \tag{2.3}$$

The thermal losses of the collector are calculated by many ways, by using different reference temperatures in every case. Eqs. (2.4)–(2.6) present these ways:

$$Q_{loss} = U_L\cdot A_{ro}\cdot\left(T_r - T_{am}\right), \tag{2.4}$$

$$Q_{loss} = \frac{\sigma\cdot A_{ro}\cdot\left(T_r^4 - T_c^4\right)}{\frac{1}{\varepsilon_r} + \frac{1-\varepsilon_c}{\varepsilon_c}\cdot\frac{A_{ro}}{A_{ci}}}, \tag{2.5}$$

$$Q_{loss} = A_{co}\cdot h_{ca}\cdot\left(T_c - T_{am}\right) + \varepsilon_c\cdot A_{co}\cdot\sigma\cdot\left(T_c^4 - T_{am}^4\right), \tag{2.6}$$

In this study, Eq. (2.4) is used because Solidworks gives as output the thermal losses and the receiver mean temperature are. The way for calculating the tube and the cover surface are presented in Eq. (2.7):

$$A_i = \pi\cdot D_i\cdot L, \tag{2.7}$$

where $i = D_{co}, D_{ci}, D_{ro}, D_{ri}$.

The convection coefficient between pressurized water and receiver is an important parameter which affects the efficiency of the system. The theoretical calculation of this is done by calculating the Nusselt number. According to literature Nusselt has different values in different flow conditions. More specifically, for laminar flow inside the tube, which means that the Reynolds number is lower than 2300; the mean Nusselt number is given by the Eq. (2.8) which is presented by Hausen [47]:

$$Nu_m = 3.66 + \frac{0.0668\cdot Re\cdot \mathrm{Pr}\cdot D_{ri}/L}{1 + 0.04\cdot\left(Re\cdot \mathrm{Pr}\cdot D_{ri}/L\right)^{2/3}}, \tag{2.8}$$

This equation has the assumption of an isothermal tube which is not quite accurate under our circumstances but it is a very close approximation. Furthermore, a comparison will prove how this model is satisfying for PTC simulation.

And for turbulent flow which means Reynolds number greater than 4000, the Colburn [47] equation gives the Nusselt Number as:

$$Nu_m = 0.023\cdot Re^{0.8}\cdot \mathrm{Pr}^{1/3}, \tag{2.9}$$

The Nusselt number is correlated with the convection coefficient according to the Eq. (2.10):

$$Nu_m = \frac{h\cdot D_{ri}}{k}, \tag{2.10}$$

Also, it is essential to be referred the equation of the Reynolds number. This number is determined by the flow conditions (temperature and velocity) and geometry (tube inner diameter). Eq. (2.11) presents Reynolds number for the tube internal flow:

$$Re = \frac{4\cdot\dot{m}}{\pi\cdot D_{ri}\cdot\mu}, \tag{2.11}$$

Eq. (2.12) presents the way that the convection coefficient is calculated. The proper data are taken from the simulation for every case and the coefficient is calculated by the Eq. (2.12):

$$h_w = \frac{Q_u}{\left(\pi\cdot D_{ri}\cdot L\right)\cdot\left(T_r - T_{fm}\right)}, \tag{2.12}$$

where the T_{fm} is the mean temperature of the water inside the tube and can be approximately calculated by Eq. (2.13) because the tube is not very long:

$$T_{fm} = \frac{T_{out} + T_{in}}{2}, \tag{2.13}$$

Another equation which is very useful at calculations is the local concentration ratio. More specifically this quantity is the absorbed irradiation in every part of the absorber to the theoretical absorbed irradiation for uniform distribution. Eq. (2.14) presents this quantity:

$$C_L = \frac{dQ_{abs}}{\rho \cdot (\tau\alpha) \cdot G \cdot dA}, \tag{2.14}$$

Finally the optical efficiency modifier is given by the next equation:

$$K(\theta) = \frac{\eta_{opt}(\theta)}{\eta_{opt}(\theta = 0^\circ)}, \tag{2.15}$$

where θ is the angular displacement in longitudinal direction.

2.3. Simulation in Solidworks

The PTC model designed in Solidworks and simulated in Flow Simulation environment. The proper boundary conditions determination is vital for the analysis. The basic boundary conditions of this problem are the following:

a. The inlet mass flow rate and the corresponding inlet Temperature. The flow is assumed to be fully developed in the inlet.
b. The pressure in the outlet.
c. The heat convection between cover outer surface and environment.

The next important part of the simulation is the determination of the radiative surfaces. Three are the main radiative surfaces of this problem:

a. The selective absorber outer surface.
b. The cover surfaces (inner and outer).

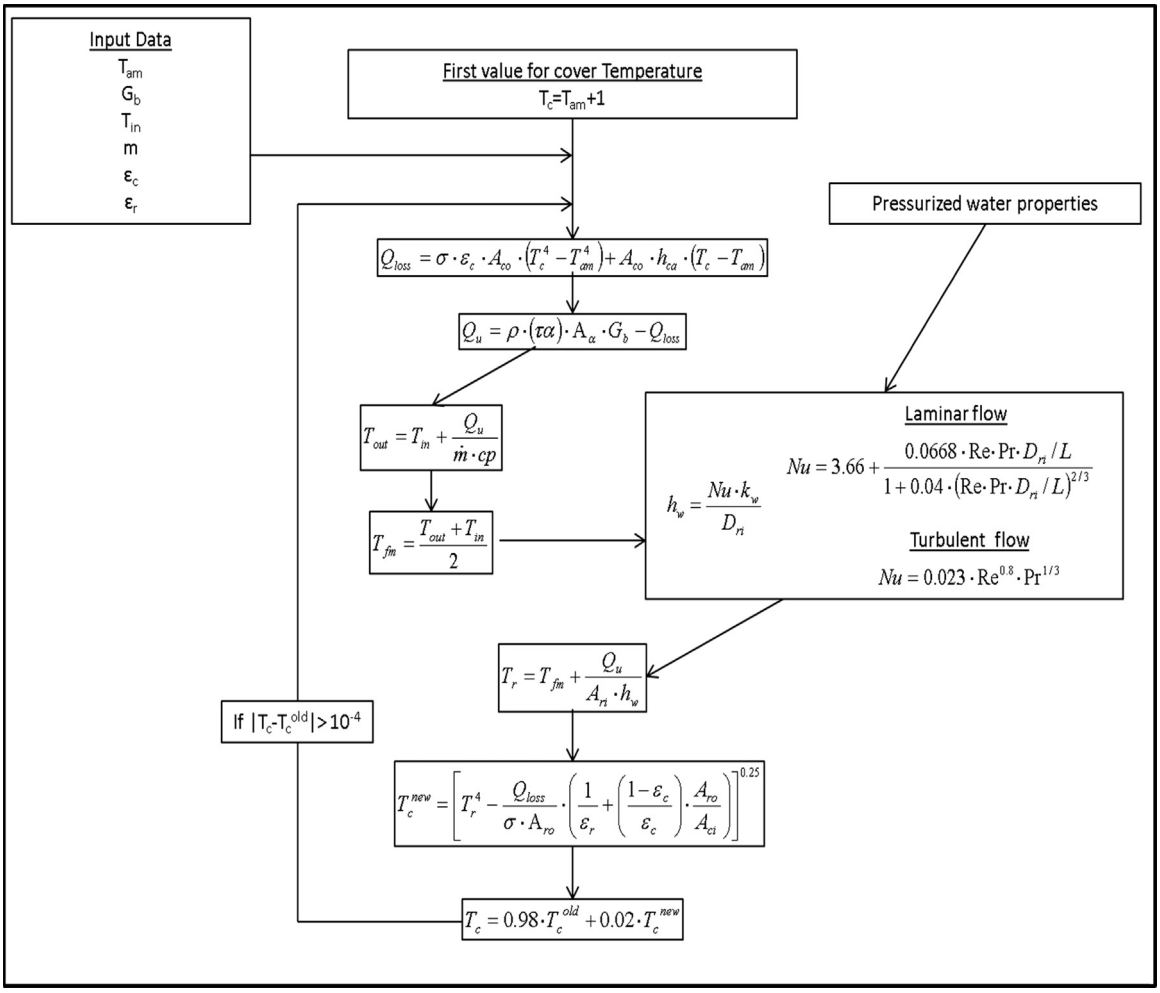

Fig. 2. Flow chart of numerical model.

c. The reflector surface that was set as “symmetry” surface in order to reflect the solar rays.

The materials for every component can be selected separately in Solidworks. So it is essential to state that:

a. The absorber tube is made of copper.
b. The cover is from glass.
c. The lids in the inlet and in the outlet are from insulation materials (insulators) in order not to take part in the thermal analysis. It is important to state that the lids are placed in the model in order to determine the fluid domain.

The outputs from Solidworks in every case are selected by the user. The fluid bulk temperature in the outlet, the mean receiver temperature, the cover mean temperature and the thermal losses of the receiver are the set of output parameters which are taken in every study-case. The mesh of the analysis is made by Solidworks and emphasis is given to the fluid cells refinement as much as in the partial cells refinement. The working fluid is pressurized water in order to keep the liquid phase of it for high temperature levels and their properties are taken by Solidworks data base.

2.4. Numerical simulation

A simple 1-D numerical model with FORTRAN was developed for validating the simulation results. The core of this model is the energy balance in the absorber in order to determine the useful energy and the heat losses. The receiver and the cover are supposed to have uniform temperatures in every case which is a good approximation because the length of the tube is not great and the temperature distribution is close to the mean value. More specifically, the flow chart of the method that was followed is given in the next figure (Fig. 2).

In the first iteration, the cover temperature was set to be greater that the ambient in order the heat transfer mechanism to be realistic. The heat losses and the useful energy are calculated in order to predict the water outlet temperature. By calculating the heat transfer coefficient between water and tube, the receiver temperature is able to be determined. The knowledge of this temperature leads to calculation of cover temperature. In order this method to be converged; a great relaxation factor was used. In most cases, 20 iterations was the computational cost in order to predict the suitable cover temperature.

The properties of water were taken from Solidworks database in order to make a better comparison between the two methods. The only property that was calculated by a literature approximation was the dynamic viscosity μ [48], with a good accordance with the Solidworks data. The heat transfer coefficient between water and tube was calculated from Eqs. (2.7) and (2.8) according the flow chart. In the numerical model, for the transient region, a linear combination of these two equations was used, something that differs from Solidworks simulation. Moreover, the use of uniform temperature for the receiver and the cover renders an important difference with Solidworks simulation.

3. Simulation results

In this paragraph the results of the simulation are presented. In every case the fluid temperature was set by the user and the other parameters, such as outlet temperature, cover mean temperature and absorber mean temperature were calculated. The solar radiation intensity and the ambient temperature were constant, as are described in Table 1. First of all the main efficiency parameters are presented.

3.1. Performance of the collector

The efficiency curve of the collector is shown in Fig. 3. In this case the solar irradiation is vertical to the aperture which

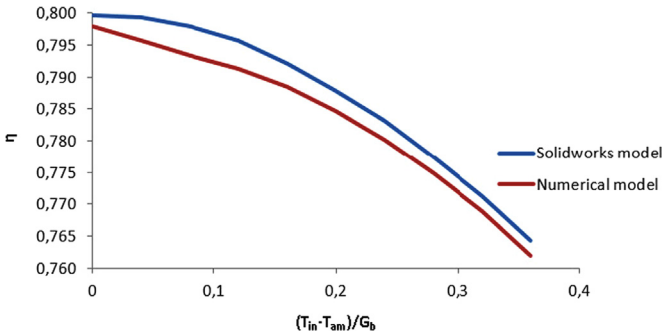

Fig. 3. Efficiency curve of the collector and comparison with the numerical model.

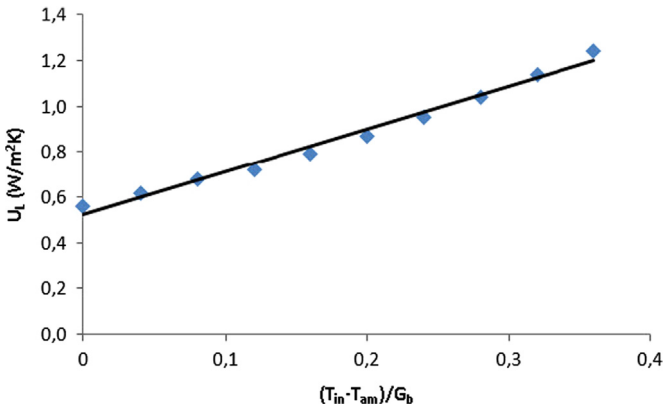

Fig. 4. Thermal losses coefficient of the collector for different operating conditions. (For interpretation of the references to color in this figure, the reader is referred to the web version of this article.)

means zero incident angle. In this case, the optical efficiency is maximum.

The comparison between the two lines shows that the numerical model gives close enough results with the simulation tool. It is important to state that efficiency is very high which proves that a PTC is able to produce water in high temperature levels efficiently. More specifically, the efficiency is greater than 75% for all the operating conditions which proves high performance of the collector.

Fig. 4 shows the total thermal loss coefficient of the absorber. This parameter is depended on the temperature because the radiation losses are greater with higher operating temperature. The correlation of this coefficient to the parameter $(T_{in}-T_{am})/G_b$ seems to be linear according to Fig. 4:

The blue points are the calculated results and the black line is a linear approximation. It is observed that this coefficient has low values which can be explained by the selective coating and the vacuum between absorber and cover. More specifically, the loss coefficient is ranges from 0.6 W/m^{2}K to 1.3 W/m^{2}K which are low values and prove the low heat losses. Fig. 5 shows the heat transfer coefficient inside the tube for different operating conditions. By changing the fluid temperature, water properties, especially dynamic viscosity (μ), change a lot. This leads the Reynolds number to be affected, according to the Eq. (2.11) and the flow varies from laminar to turbulent, while there is a transitional region according the next diagram:

Reynolds number in the right axis determines the kind of the flow inside the tube. While the mass flow rate is constant, Reynolds number changes because of changing the water inlet temperature. It is essential to state that laminar flow is conjugated with lower heat transfer coefficient (about 300 W/m^{2}K) while turbulent gives greater values of this (1000 W/m^{2}K). This proves the better heat transfer conditions of the turbulent flow. In the transitional region the heat coefficient takes an intermediate value according to the Fig. 5. The blue line shows the calculation according to the solidworks results and the red line gives the convection coefficient according to the theoretical models of Eqs. (2.7) and (2.8) for the respect temperatures of the water in the inlet. The results are very close to each other fact that validates the Solidworks results. This proves the better heat transfer conditions of the turbulent flow.

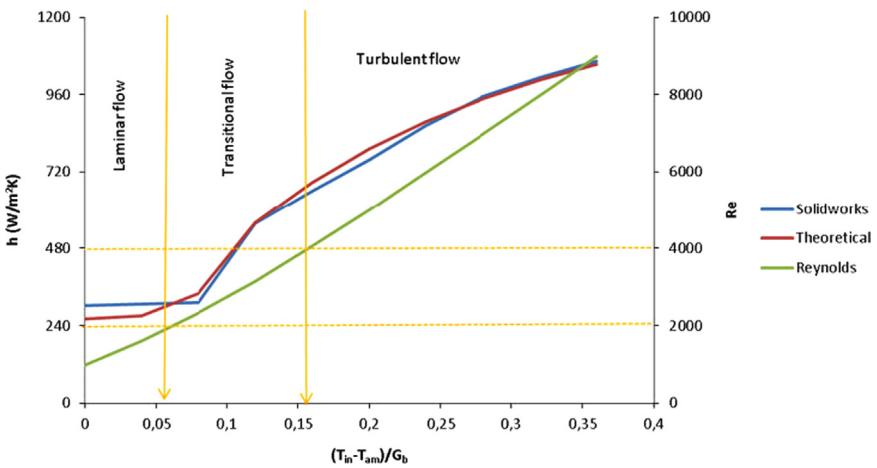

Fig. 5. Heat convection coefficient and Reynolds number for different operating conditions. (For interpretation of the references to color in this figure, the reader is referred to the web version of this article.)

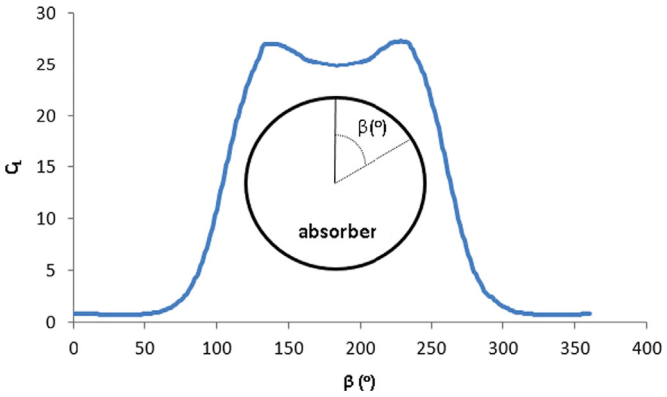

Fig. 6. Local concentration ratio in the absorber surface.

Fig. 6 shows the local concentration ratio in the absorber. The scheme inside the figure shows how the angle β is determined.

The distribution of this parameter is symmetrical because the sun rays are vertical to the aperture. For low values of angle β, the concentration ratio has values lower to 1, because no reflected rays reach there. For greater values, the concentration ratio is increasing, specifically at 135° it is about 27 but at 180° it is diminished to 25. This is happening because the rays are concentrated in the bottom of the absorber and specifically the maximum value is in the sides of the lower part. The mean value of the concentration ration is 12.15 which is near to the mean value of the maximum and minimum value of the local concentration ratio.

Fig. 7 shows the incident angle modifier of the optical efficiency. When the sun changes position, the angle of rays differs, something that affects the rays' reflections. This was simulated by changing the direction of beam radiation in general settings. This parameter is given in Fig. 7 and is a very useful parameter for daily simulation of this collector.

The optical efficiency is reduced for greater values of incident angle and for angles greater than 70°, no rays arrive to the receiver after the reflections. For incident angles up to 20°, the optical efficiency modifier is greater than 0.8 which leads to an acceptable efficiency. For this reason a tracking system for this collector is needed in order to keep the incident angle in low levels.

Table 2 presents equations which approaches the presented curves. In addition, important parameters of the collector are given in order the analysis to be completed.

The thermal efficiency is a 2nd degree polynomial which is explained by the linear dependence of losses coefficient by the fluid temperature.

3.2. Distribution over the geometry

In this section some figures which give the temperature and heat flux distribution over the geometry are presented. The water inlet temperature is at 90 °C in all the following figures. These results are output from Solidworks and the images are taken from its environment. The water distribution in the outlet is shown in Fig. 8 which follows:

The fluid is warmer in the bottom of the tube because the rays are concentrated on the respective part of the absorber. The center part of the tube is colder because the peripheral water is heated from the hot tube and after that the heat is transferred by conduction inside the tube.

Fig. 9 is consisted of two parts. The upper part presents the water temperature profile for 5 different positions inside the

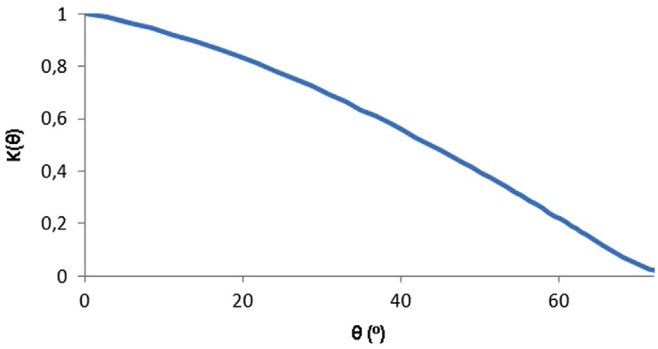

Fig. 7. Optical efficiency modifier for different angular values.

Table 2
Final simulation results.

$\eta = 0.8 - 0.008843 \cdot \left(\frac{T_{in} - T_{am}}{G_b}\right) - 0.00050558 \cdot G_b \cdot \left(\frac{T_{in} - T_{am}}{G_b}\right)^2$
$U_L = 0.5222 + 1.8773 \cdot \left(\frac{T_{in} - T_{am}}{G_b}\right)$
$K(\theta) = 1.0159 - 0.448 \cdot \theta - 0.2985 \cdot \theta^2$
$F_R = 0.9981\ F' = 0.9984\ F'' = 0.9997$

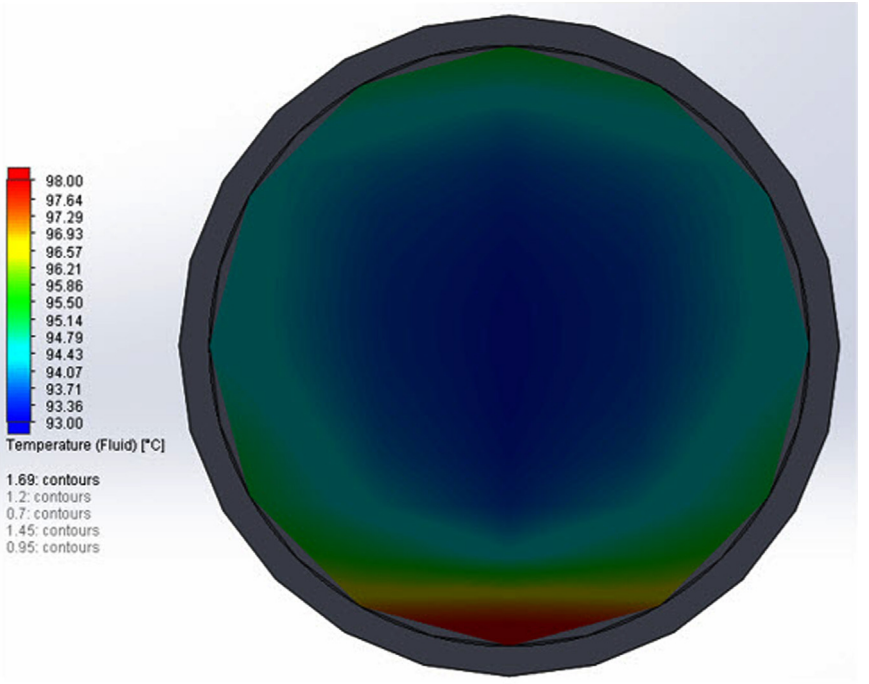

Fig. 8. Fluid temperature distribution in the outlet of the tube from Solidworks, with red color is the warmer part of the water. (For interpretation of the references to color in this figure legend, the reader is referred to the web version of this article.)

tube and the other the temperature distribution in the absorber surface along the tube.

The red color shows the warmer parts of the schemes in the Fig. 9. According to the part “a” the water is coming warmer while it flows along the tube and especially the lower part is the hottest part of all the tube. The part “b” presents the absorber temperature and it is obvious that the lower part is the warmer part. The concentration of solar rays in this area leads the temperature to be higher and to create a non-isothermal tube. Fig. 10 shows the distribution of temperature in the absorber surface in a cross section at 70% of the total length.

The maximum value is observed in the bottom of the tube where the radiation is concentrated. This distribution is symmetrical and the difference between the maximum and the minimum temperature is about 3 K. The following figure shows the heat flux distribution over the absorber surface. With the blue color are the greater values and with red the lower. The negative sign in the legend values has not a physical importance (Fig. 11).

The solar radiation is concentrated on the lower part of the tube and especially in the sides of the lower part. The dimensions of the model determine the exact distribution of the heat flux.

It is obvious that Solidworks flow simulation is able to simulate concentrating solar collectors by an easy way and gives many features to the users. All the important parameters of the collector's efficiency have been presented in this paragraph, as the thermal efficiency curve, the incident angle modifier of optical efficiency and the thermal loss coefficient. The calculation of the temperature distribution over the tube surface and of the water in every position is very important and it is able to be made by Solidworks. Also, the heat flux distribution over the receiver is able to be calculated in every position by the features of the simulation tool gives. By this way, the user is able know all the quantities in every position of the model.

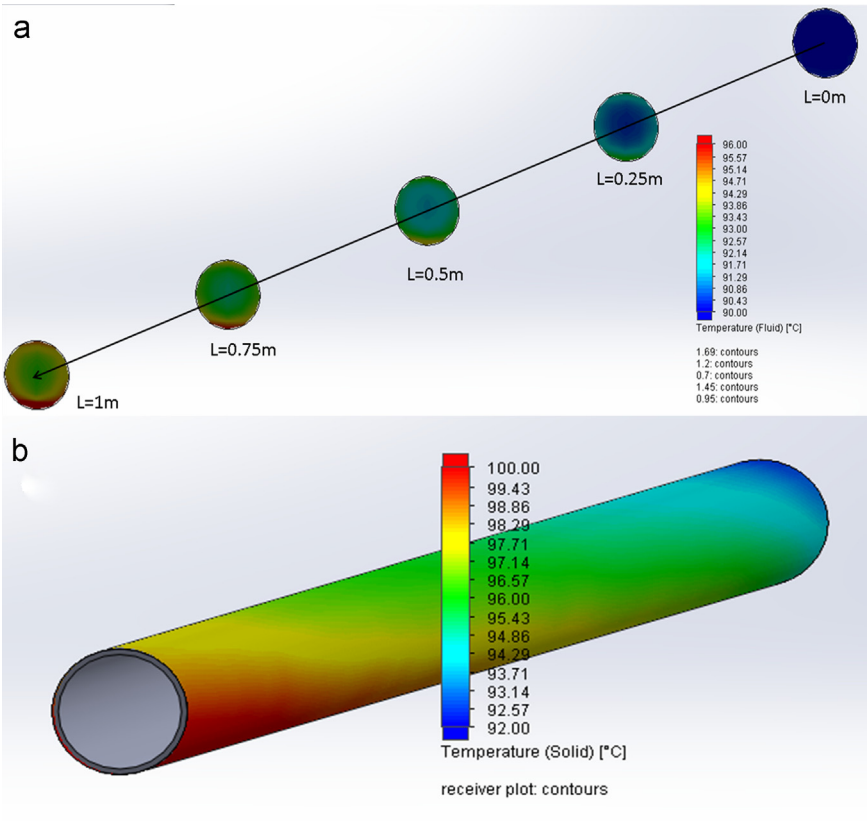

Fig. 9. Temperature distribution from Solidworks: (a) of the water in 5 different positions along the tube and (b) in the absorber surface. (For interpretation of the references to color in this figure legend, the reader is referred to the web version of this article.)

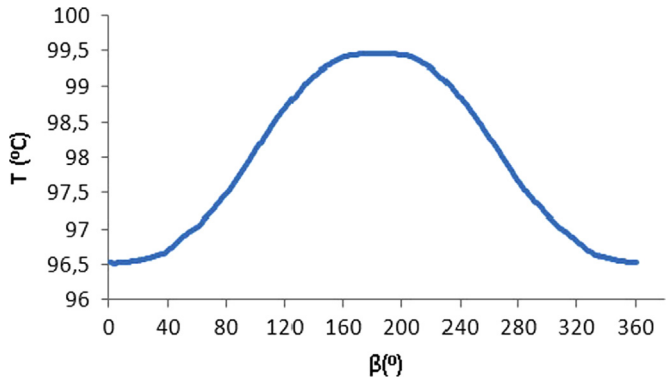

Fig. 10. Temperature absorber distribution in the peripheral line in the 70% of the length.

4. Conclusions

In this study, a simulation of a parabolic trough collector by the commercial software Solidworks is presented. The results are validated by a simple numerical model which was developed by the laboratory. The final results of the simulation are at good proximity with the numerical model. Emphasis is given on the calculation of the working fluid convection coefficient and for this reason a validation with the theoretical value is presented. Moreover, it is proved that Solidworks gives great features to the users, because it allows the knowledge of all calculated quantities in every position of the model. Also, the presented numerical model is innovative and leads to accurate results with low computational cost. The relaxation factor is the key point of this model in order the method to be converged.

The efficiency of the collector is over 75% for high temperature levels, a fact that renders this technology beneficial. This high efficiency can be explained by the very low heat loss coefficient which varies from 0.6 to 1.3 W/m^2K, depending on the inlet temperature. The next important parameter investigated is the solar heat flux distribution over the absorber surface

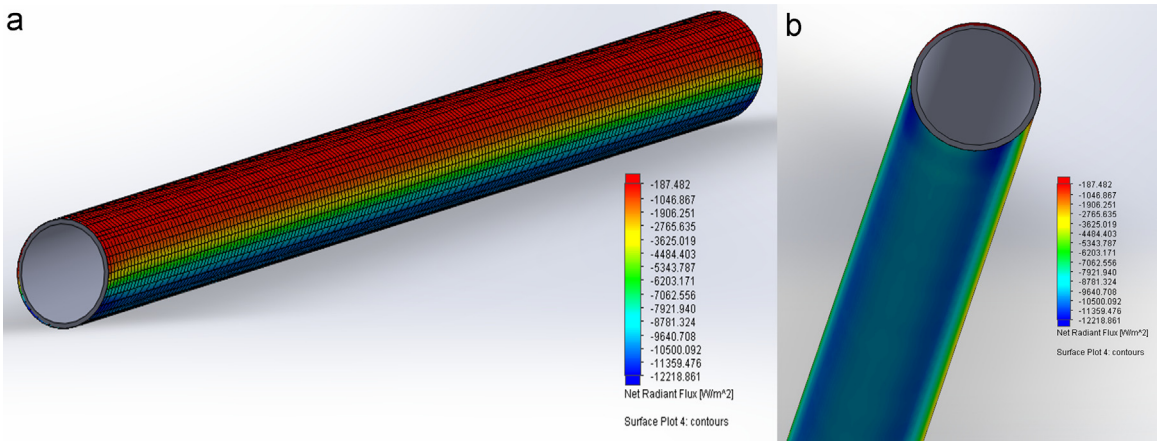

Fig. 11. Heat flux distribution from Solidworks: (a) for the upper part of the tube and (b) for the lower part of the tube. (For interpretation of the references to color in this figure, the reader is referred to the web version of this article.)

because this parameter affects the temperature distribution of the absorber. The solar energy is concentrated on the lower part of the absorber with the maximum concentration ratio to be observed at 45° from vertical direction. Moreover, the maximum local concentration ratio is about 27, the mean 12.15 while the upper part concentration ratio is close to one.

The heat flux concentration distribution determines the temperature distribution over the absorber; thus the down part of it is the warmer one. More specifically, the temperature variation in the peripheral of the absorber is about 3 K degrees which proves that the temperature distribution is no uniform. The temperature distribution of the water in a cross section shows that the fluid is warmer in the down part, because the absorber is warmer in the respective part.

The analysis of the heat convection coefficient inside the tube concludes that the Reynolds number is fully dependent on the water inlet temperature. This means that in low temperature level the flow is laminar with a convection coefficient about 300 W/m^2K and for higher temperature levels the flow becomes turbulent with a greater convection coefficient about 1000 W/m^2K.

The solar radiation direction is very important for the efficiency of the collector and especially for its optical part. A greater incident angle creates higher end losses in the collector which affects the efficiency. When the incident angle, in the longitude direction, is up to 20°, the angle efficiency modifier is greater than 0.8 and the collector performance is high. After 70°, the solar energy that reaches to the absorber is not sufficient for producing useful energy and the collector is not able to operate.

Finally, it is important to state, that the determination of the thermal efficiency equation and the optical modifier equation gives to the user the ability to know the performance of the collector in various operating conditions. As a result, the input of this model, through these equations, in another simulation tool or code can be easily achieved.

References

[1] K. Nithyanandam, R. Pitchumani, Optimization of an encapsulated phase change material thermal energy storage system, Sol. Energy 107 (2014) 770–788.
[2] N.S. Suresh, N.C. Thirumalai, Badri S. Rao, M.A. Ramaswamy, Methodology for sizing the solar field for parabolic trough technology with thermal storage and hybridization, Sol. Energy 110 (2014) 247–259.
[3] Gur Mittelman, Michael Epstein, A novel power block for CSP systems, Sol. Energy 84 (10) (2010) 1761–1771.
[4] A. Fernández-García, E. Zarza, L. Valenzuela, M. Pérez, Parabolic-trough solar collectors and their applications, Renew. Sustain. Energy Rev. 14 (2010) 1695–1721.
[5] K. Zabara, Estimation of the global solar radiation in Greece, Sol. Wind Technol. 3 (4) (1986) 267–272.
[6] D.A. Kouremenos, K.A. Antonopoulos, E.S. Domazakis, Solar radiation correlations for the Athens, Greece, area, Sol. Energy. 35 (3) (1985) 259–269.
[7] D. Kruger, Y. Pandian, et al., Parabolic trough collector testing in the frame of the REACt project, Desalination 220 (1–3) (2008) 612–618.
[8] R. Grena, Optical simulation of a parabolic solar trough collector, Int. J. Sustain. Energy 29 (1) (2010) 19–36.
[9]] H. Price, E. Lópfert, D. Kearney, E. Zarza, G. Cohen, R. Gee, et al., Advances in parabolic trough solar power technology, J. Sol. Energy Eng. 124 (2002) 109–125.
[10] Marco Binotti, Guangdong Zhu, Allison Gray, Giampaolo Manzolini, Paolo Silva, Geometric analysis of three-dimensional effects of parabolic trough collectors, Sol. Energy 88 (2013) 88–96.
[11] J.A. Clark, An analysis of the technical and economic performance of a parabolic trough concentrator for solar industrial process heat application, Int. J. Heat Mass Transf. 25 (9) (1982) 1427–1438.
[12] S. Al-Soud Mohammed, S. Hrayshat Eyad, A 50 MW concentrating solar power plant for Jordan, J. Clean. prod. 17 (2009) 625–635.
[13] N. El Gharbi, H. Derbal, S. Bouaichaoui, N. Said, A comparative study between parabolic trough collector and linear Fresnel reflector technologies, Energy Proc. 6 (2011) 565–572.
[14] T. Boukelia, M.S. Mecibah, Parabolic trough solar thermal power plant: potential, and projects development in Algeria, Renew. Sustain. Energy Rev. 21 (2013) 288–297.
[15] W. Grasse, Solar PACES Annual Report, DLR, Germany, 1995.
[16] Malika Ouagued, Abdallah Khellaf, Larbi Loukarfi, Estimation of the temperature, heat gain and heat loss by solar parabolic trough collector under

Algerian climate using different thermal oils, Energy Convers. Manag. 75 (2013) 191–201.
[17] Ze-Dong Cheng, Ya-Ling He, Bao-Cun Du, Kun Wang, Qi Liang, Geometric optimization on optical performance of parabolic trough solar collector systems using particle swarm optimization algorithm, Appl. Energy 148 (2015) 282–293.
[18] A. de Risi, M. Milanese, D. Laforgia, Modelling and optimization of transparent parabolic trough collector based on gas-phase nanofluids, Renew. Energy 58 (2013) 134–139. October.
[19] A. Hachicha, I. Rodríguez, O. Lehmkuhl, A. Oliva, On the CFD&HT of the flow around a parabolic trough solar collector under real working conditions, Energy Proc. 49 (2014) 1379–1390.
[20] Z.D. Cheng, Y.L. He, F.Q. Cui, B.C. Du, Z.J. Zheng, Y. Xu, Comparative and sensitive analysis for parabolic trough solar collectors with a detailed Monte Carlo ray tracing optical model, Appl. Energy 115 (15) (2014) 559–572.
[21] T. Sokhansefat, A.B. Kasaeian, F. Kowsary, Heat transfer enhancement in parabolic trough collector tube using Al_2O_3/synthetic oil nanofluid, Renew. Sustain. Energy Rev. 33 (2014) 636–644.
[22] Hongbo Liang, Shijun You, Huan Zhang, Comparison of different heat transfer models for parabolic trough solar collectors, Appl. Energy 148 (2015) 105–114.
[23] Fritz Zaversky, Rodrigo Medina, Javier García-Barberena, Marcelino Sánchez, David Astrain, Object-oriented modeling for the transient performance simulation of parabolic trough collectors using molten salt as heat transfer fluid, Sol. Energy 95 (2013) 192–215.
[24] Ze-Dong Cheng, Ya-Ling He, Yu Qiu, A detailed nonuniform thermal model of a parabolic trough solar receiver with two halves and two inactive ends, Renew. Energy 74 (2015) 139–147.
[25] G.J. Gong, X.Y. Huang, J. Wang, M.L. Hao, An optimized model and test of the China's first high temperature parabolic trough solar receiver, Sol. Energy 84 (2010) 2230–2245.
[26] Acine Marif, Hocine Benmoussa, Hamza Bouguettaia, Mohamed M. Belhadj, Moussa Zerrouki, Numerical simulation of solar parabolic trough collector performance in the Algeria Saharan region, Energy Convers. Manag. 85 (2014) 521–529.
[27] Yanjuan Wang, Qibin Liu, Jing Lei, Hongguang Jin, Performance analysis of a parabolic trough solar collector with non-uniform solar flux conditions, Int. J. Heat Mass Transf. 82 (2015) 236–249.
[28] Ze-Dong Cheng, Ya-Ling He, Kun Wang, Bao-Cun Du, F.Q. Cui, A detailed parameter study on the comprehensive characteristics and performance of a parabolic trough solar collector system, Appl. Therm. Eng. 63 (2014) 278–289.
[29] Yanjuan Wang, Qibin Liu, Jing Lei, Hongguang Jin, A three-dimensional simulation of a parabolic trough solar collector system using molten salt as heat transfer fluid, Appl. Therm. Eng. 70 (2014) 462–476.
[30] M. Eck, J.F. Feldhoff, R. Uhlig, Thermal modelling and simulation of parabolic trough receiver tubes, in: Proceedings of the ASME 2010 4th International Conference on Energy Sustainability, Phoenix, 2010.
[31] Li Xu, Zhifeng Wang, Xin Li, Guofeng Yuan, Feihu Sun, Dongqiang Lei, Dynamic test model for the transient thermal performance of parabolic trough solar collectors, Sol. Energy 95 (2013) 65–78.
[32] Esmail M.A. Mokheimer, Yousef N. Dabwan, Mohamed A. Habib, Syed A.M. Said, Fahad A. Al-Sulaiman, Techno-economic performance analysis of parabolic trough collector in Dhahran, Energy Convers. Manag. 86 (2014) 622–633.
[33] İbrahim Halil Yılmaz, Mehmet Sait Söylemez, Thermo-mathematical modeling of parabolic trough collector, Energy Convers. Manag. 88 (2014) 768–784.
[34] Soteris A. Kalogirou, A detailed thermal model of a parabolic trough collector receiver, Energy 48 (1) (2012) 298–306.
[35] Chung-Yu Tsai, Psang Dain Lin, Optimized variable-focus-parabolic-trough reflector for solar thermal concentrator system, Sol. Energy 86 (5) (2012) 1164–1172.
[36] S.M. Akbarimoosavi, M. Yaghoubi, 3D Thermal-structural Analysis of an Absorber Tube of a Parabolic Trough Collector and the Effect of Tube Deflection on Optical Efficiency, Energy Proc. 49 (2014) 2433–2443.
[37] P. Mohammad Zadeh, T. Sokhansefat, A.B. Kasaeian, F. Kowsary, A. Akbarzadeh, Hybrid optimization algorithm for thermal analysis in a solar parabolic trough collector based on nanofluid, Energy 82 (2015) 857–864.
[38] Ya-Ling He, Jie Xiao, Ze-Dong Cheng, Yu-Bing Tao, A MCRT and FVM coupled simulation method for energy conversion process in parabolic trough solar collector, Renew. Energy 36 (2011) 976–985.
[39] Z.D. Cheng, Y.L. He, J. Xiao, Y.B. Tao, R.J. Xu, Three-dimensional numerical study of heat transfer characteristics in the receiver tube of parabolic trough solar collector, Int. Commun. Heat Mass Transf. 37 (2010) 782–787.
[40] Aggrey Mwesigye, Tunde Bello-Ochende, Josua P. Meyer, Heat transfer and thermodynamic performance of a parabolic trough receiver with centrally placed perforated plate inserts, Appl. Energy 136 (2014) 989–1003.
[41] Victor C. Pigozzo Filho, Alexandre B. de Sá, J.úlio C. Passos, Sergio Colle, Experimental and Numerical Analysis of Thermal Losses of a Parabolic Trough Solar Collector, Energy Proc. 57 (2014) 381–390.
[42] Liang Zhang, Zitao Yu, Liwu Fan, Wujun Wang, Huan Chen, Yacai Hu, Jianren Fan, Mingjiang Ni, Kefa Cen, An experimental investigation of the heat losses of a U-type solar heat pipe receiver of a parabolic trough collector-based natural circulation steam generation system, Renew. Energy 57 (2013) 262–268.
[43] Liang Zhang, Wujun Wang, Zitao Yu, Liwu Fan, Yacai Hu, Yu Ni, Jianren Fan, Kefa Cen, An experimental investigation of a natural circulation heat pipe system applied to a parabolic trough solar collector steam generation system, Sol. Energy 86 (2012) 911–919.
[44] X. Xiao, P. Zhang, D.D. Shao, M. Li, Experimental and numerical heat transfer analysis of a V-cavity absorber for linear parabolic trough solar collector, Energy Convers. Manag. 86 (2014) 49–59.
[45] Loreto Valenzuela, Rafael López-Martín, Eduardo Zarza, Optical and thermal performance of large-size parabolic-trough solar collectors from outdoor experiments: a test method and a case study, Energy 70 (2014) 456–464.
[46] V.E. Dudley, G.J. Kolb, M. Sloan, D. Kearney, Test Results: SEGS LS-2 Solar Collector, Report of Sandia National Laboratories (SAND94-1884), 1994.
[47] J. Leinhard IV, J. Leinhard V, A Heat Tranfer Textbook, 4th edition . Philogiston Press, USA, 2012, 354–360.
[48] Tarik Al-Shemmeri, Engineering Fluid Mechnanics, Ventus Publishing ApS, Denmark, 2012, 17–18.